Int. J. Heat Mass Transfer. Vol. 26, No. 10, pp. 1463–1477, 1983
Printed in Great Britain

0017-9310/83 $3.00 + 0.00

PREDICTION OF CRITICAL HEAT FLUX IN FLOW BOILING AT LOW QUALITIES

J. WEISMAN and B. S. PEI*
Department of Chemical & Nuclear Engineering, University of Cincinnati, Cincinnati, OH 45221, U.S.A.

(*Received* 2 *April* 1982 *and in revised form* 24 *January* 1983)

Abstract—A theoretically based prediction of CHF has been developed for high velocity flow in tubes. Turbulent interchange between the bubbly layer and core regions is taken as the limiting mechanism. Good agreement was obtained between predictions and experimental data for water flowing in uniformly and non-uniformly heated tubes. The predictive procedure developed for water was found to yield results in agreement with experiment for each of the four other fluids examined.

NOMENCLATURE

a	two phase multiplier in turbulent intensity equation
A	total cross sectional flow area [length^2]
A_2	cross-sectional flow area in bubbly layer [length^2]
D	tube diameter, [length]
D_h	hydraulic diameter [length]
D_p	average bubble diameter [length]
f'	friction factor
$f(v')$	distribution function for v'
F	axial heat flux distribution correlation factor in W-3 correlation
F_1, F_2	unknown functional relationships
G	total axial mass velocity [mass/(length^2 time)]
G_3	lateral mass velocity from core to bubbly layer due to turbulence [mass/(length^2 time)]
g_c	gravitational conversion factor [(mass-length)/(force) (time^2)]
h_f	saturated liquid enthalpy [energy/mass]
h_{fg}	evaporation enthalpy change [energy/mass]
h_l	enthalpy of liquid [energy/mass]
h_{ld}	enthalpy at point of bubble detachment [energy/mass]
H_0	constant, 270 [h^{-1} °C^{-1}]
$H_{1\phi}$	single phase heat transfer coefficient
i_b	turbulent intensity at bubbly layer core interface
k	constant
k_l	liquid conductivity [energy/time length degree)]
l_e	Prandtl mixing length [length]
$\dot{m}_1$	axial mass flow rate in core [mass/time]
$\dot{m}_2$	axial mass flow rate in bubbly layer [mass/time]
$\dot{m}_3$	lateral mass flow rate from core to bubbly layer [mass/time]
$\dot{m}_4$	lateral mass flow rate from core to bubbly layer [mass/time]
$\dot{m}_t$	total axial mass flow rate [mass/time]
Nu	Nusselt number
Pr	Prandtl number
p_H	heated perimeter [length]
q''	total heat flux [energy/(length^2 time)]
q''_b	that portion of total heat flux effective in generating vapor [energy/(length^2 time)]
q''_{cond}	heat flux due to bubble condensation [energy/(length^2 time)]
q''_{DNB}	DNB heat flux [energy/(length^2 time)]
r	radial position [length]
r_0	outer radius of tube [length]
R	(predicted critical heat flux)/(measured critical heat flux)
Re	Reynolds number
s	bubbly layer thickness [length]
U_τ	frictional velocity [length/time]
$\bar{V}$	global velocity of two-phase mixture [length/time]
V_1	average axial velocity of bulk flow [length/time]
V_2	average axial velocity of bubbly layer [length/time]
v_{11}	radial velocity created by vapor generation [length/time]
v'	radial fluctuating velocity [length/time]
$\tilde{v}'$	mean value of v'
$\overline{v'^2}^{1/2}$	root mean square value of v'
x_1	average quality in core region
x_2	average quality in bubbly layer
x_{avg}	$\langle x \rangle$ = global quality
y	distance from wall, $r_0 - r$ [length]
z	axial distance [length]
z_{CHF}	axial distance at which CHF occurs [length]

Greek symbols

α_1	average void fraction in core
α_2	average void fraction in bubbly layer
$\langle\alpha\rangle$	average void fraction (across entire cross section)
α_{CHF}	void fraction of bubbly layer at CHF
ψ	$\left\{\frac{1}{2\pi}\exp-\left[-\frac{1}{2}\left(\frac{v_{11}}{\sigma_{v'}}\right)^2 1 - \frac{1}{2}\left(\frac{v_{11}}{\sigma_{v'}}\right)\mathrm{erfc}\left(\frac{1}{\sqrt{2}}\frac{v_{11}}{\sigma_{v'}}\right)\right\}\right.$

* Present address: Tsing Hua University, Hinshu, Taiwan.

ρ_l	liquid density at bulk temperature [mass/length^3]
ρ_f	density of saturated liquid [mass/length^3]
ρ_g	vapor density [mass/length^3]
$\bar{\rho}$, ρ_{avg}	average density (across entire flow area) [mass/length^3]
σ	surface tension [force/length]
$\sigma_{v'}$	standard deviation of v'
$\sigma(R)$	standard deviation of R
μ_{avg}	viscosity of mixture [mass/(length time)]
μ_l	viscosity of liquid [mass/(length time)]
$\mu(R)$	mean value of R

1. INTRODUCTION

THE ACCURATE prediction of critical heat flux (CHF) in flow boiling is of importance in a wide variety of process equipment. For design purposes, such predictions are still largely made using empirical correlations having no theoretical basis.

There is general agreement that the mechanisms leading to CHF depends on the flow quality. At high qualities, the flow is annular and CHF is caused by dryout of the liquid film on the heated surface. It is generally agreed that such dryout can be predicted by appropriate modeling of vaporization plus entrainment from, and droplet deposition on, the annular liquid film. Several theoretically based prediction approaches, the most recent being that of Levy *et al.* [1], have been applied with relatively good success.

CHF at low qualities occurs when the bubbles near the wall coalesce into a vapor film. Although a number of theoretically based correlations have been proposed for low quality CHF, none of these has been entirely satisfactory. Thorgerson *et al.* [2] have suggested that the critical heat flux is related to a critical friction factor. By using the Reynolds analogy, they obtained the critical heat flux in terms of the friction factor, temperature difference and fluid velocity at CHF. Thorgerson *et al.* were able to correlate their own low pressure data but were unable to extend the correlation to other data. Bergles [3] has pointed out that this method would not be a very useful predictive technique since it requires the critical pressure drop which must be determined by the same experiment in which CHF is measured.

Several correlations [4–7] have been based on the general idea that the pool-boiling critical heat flux, with subcooling effects, can be added to the heat flux for single phase flow at the burnout wall temperature. Expression of this type can give an acceptable correlation of data since they generally contain a number of adjustable constants. However, they do not shed any light on the mechanism of subcooled boiling burnout.

Fiori and Bergles [8] postulated that, in slug flow, the critical heat flux condition is caused by dryout of a microfilm under a vapor clot. While this suggestion appears to be in accord with their visual observations and transient temperature observations, they were not able to obtain quantitative predictions from this model.

The mechanism most generally accepted as leading to CHF at low qualities is that of bubble crowding and vapor blanketing at the wall. The bubble layer near the wall is assumed to become so thick that it inhibits enthalpy transport between the fluid in the core and the liquid near the wall. In one version of this idea, it is assumed that CHF occurs when a critical superheat is reached in the liquid near the wall. Tong [9] used this idea to relate CHF under non-uniform conditions to CHF at uniform conditions but no basic CHF correlation was proposed.

Some investigators have proposed that enthalpy transport to the bubble layer is inhibited when the boundary layer separates from the wall. Kutadeladze and Leont'ev [4] used gas injection to simulate boiling and concluded that the forced convection boundary layer could be blown off the wall. They devised a complex correlation, based on this idea, which agreed with water and alcohol data over a narrow range. Tong [10] extended the work of Kutadeladze and Leont'ev [4] and obtained a simple expression for critical heat flux. The expression contained a single constant which was a complex function of quality but the actual correlation was not particularly good in the low quality range. Hancox and Nicoll [11] also used the boundary layer separation idea for the basis of a CHF correlation. However, Bergles [3] notes that the verification of the assumed mechanism is questionable since seven experimental constants were required in the final correlation.

Hebel *et al.* [12, 13] have also proposed a model based on vapor bubble obstruction of enthalpy transport. In their model, dissipation of bubbles at the wall depends on vapor condensation in the subcooled fluid and vapor transport by the flowing coolant. When the rate of bubble production at the heater wall exceeds the local vapor absorption capacity, a vapor blanket develops at the wall. In their revised model, Hebel *et al.* [13] account for flow of vapor bubbles away from the heated surface as well as the flow of liquid towards the heater surface. This correlation, which required four experimental constants, was only capable of providing a lower envelope for the data they examined.

Recently, Smogalev [14] has devised a model for estimating critical heat fluxes via a transport model. He was able to show reasonable agreement with limited experimental data for water. His model is, however, limited to subcooled water at low mass velocities; velocities below the range of industrial interest.

A number of correlations based on dimensional analysis, coupled in many cases with some consideration of the phenomena involved, have been proposed [15–17]. One of the most recent of such correlation attempts is that of Katto [18]. He divided the available CHF data into 5 regimes. Of these, portions of Katto's H and HP regimes and all of his N regime correspond to low quality CHF data. While a reasonable correlation of water data was obtained, there is no real theoretical basis for the dimensionless groups used or any

indication that the correlation would apply to fluids other than water.

In view of the foregoing, it was concluded that none of the theoretically related predictions of CHF at subcooled conditions or low qualities, available at the outset of this work, were fully adequate. This study was therefore undertaken to provide a theoretically based prediction which would provide good accuracy when applied to (a) uniformly heated water data at a variety of conditions and from a variety of sources (b) non-uniformly heated tests (c) data at the high mass velocities of industrial interest (d) CHF data obtained with fluids other than water.

2. BASIS OF PRESENT MODEL

The existence of a bubbly layer adjacent to the wall in boiling at subcooled or low quality conditions has been confirmed by a number of investigators [9, 20-23]. Fairly wide acceptance has been given to the idea that limited enthalpy transport between the bubbly layer and core leads to the critical heat flux under these subcooled and low quality conditions. Although the idea that boundary layer separation is the cause of the limited interchange it has not led to general correlations, other approaches to the establishment of the limiting interchange conditions appear promising [13]. The present work is therefore based on attempting to develop a model for the interchange between the core region and bubbly layer and relating this to the conditions at which vapor blanketing occurs.

The present model is based upon the following postulates:

(1) Under subcooled and low quality conditions, CHF is a local phenomenon. This is in accord with currently held views [2, 12, 13].

(2) During subcooled and low quality boiling, the bubbly layer builds up in thickness along the channel until it fills the region close to the wall where the turbulent eddy size is insufficient to transport the bubbles radially [24]. At the CHF location, the bubbly layer is assumed to be at this maximum thickness.

(3) CHF occurs when the volume fraction of steam in the bubbly layer just exceeds the volume fraction (critical void fraction) at which an array of ellipsoidal bubbles can be maintained without significant contact between the bubbles.

(4) The volume fraction of steam in the bubbly layer is determined by a balance between the outward flow of vapor and the inward flow of liquid at the bubbly layer–core interface. This is reasonable based on the supposition that liquid entering the bubbly layer may be taken as eventually reaching the wall. This implies that the interstices between the bubbly layer are filled with turbulent liquid and that this turbulence level is enhanced by the presence of the bubbles and the boiling process. The critical turbulent transport rate then appears at the edge of the bubbly layer where the liquid turbulence enhancement is substantially below that found within the layer.

3. MATHEMATICAL FORMULATION OF MODEL

The bubbly layer at the critical heat flux location, z_{CHF}, is shown schematically in Fig. 1. For flow of suspended particles or bubbles, Lee and Durst [24] have pointed out that the region occupied by the high concentration of bubbles or suspended particles corresponds to the region adjacent to the wall where the size of the turbulent eddies is so small that the eddies are unable to move the particles or bubbles. Particles or bubbles in this region move as if in laminar flow. Lee and Durst [24] suggested that a fully complete description of the behavior would require the use of a wall region, buffer region and core region. However, they also noted that the buffer region is very narrow and that adequate modeling could be obtained by use of only a wall and core region. We shall follow this suggestion.

While the concentration of bubbles changes sharply in the buffer region and probably in the region very close to the wall, visual observations appear to indicate little change in bubble concentration within the bulk of the bubble layer. We shall therefore assume that the quality in the bubbly layer may be taken as a constant at the average value, x_2.

In addition to the axial flow in and out of the bubbly layer control volume, there is radial interchange between the bubbly layer and the core region. If $\dot{m}_3$ represents the total flow rate from core to bubbly layer and $\dot{m}_4$ the total flow rate from bubbly layer to core, then the total mass balance on the bubbly layer is

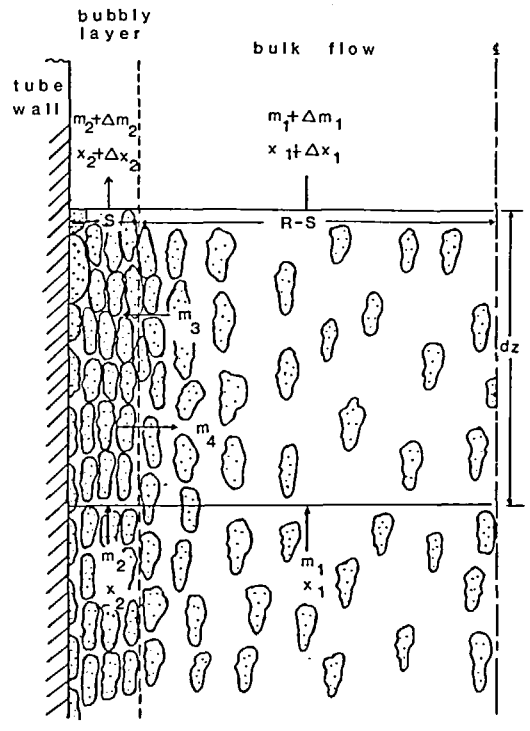

FIG. 1. Schematic diagram of transport between core and bubbly layer.

written as

$$\dot{m}_3 = \Delta\dot{m}_2 + \dot{m}_4. \quad (1)$$

A mass balance on the liquid in the bubbly layer yields

$$\dot{m}_3(1-x_1) = \frac{q''_b(2\pi r)\Delta z}{h_{fg}} - \dot{m}_2(\Delta x_2) + \Delta\dot{m}_2(1-x_2) + \dot{m}_4(1-x_2) \quad (2)$$

when second order terms are ignored.
By combining these mass balances we obtain

$$\dot{m}_3(x_2-x_1) = \frac{q''_b(2\pi r)\Delta z}{h_{fg}} - \dot{m}_2(\Delta x_2). \quad (3)$$

We may rewrite this by replacing $\dot{m}_3$ by $G_3 = 2\pi(r_0-s)\Delta z$ and then dividing by $2\pi(r_0-s)\Delta z$ and obtain

$$G_3(x_2-x_1) = \frac{q''_b}{h_{fg}}\left(\frac{r_0}{r_0-s}\right) - \frac{\dot{m}_2}{2\pi(r_0-s)}\left(\frac{\Delta x_2}{\Delta z}\right). \quad (4)$$

We simplify this by recognizing that the ratio $\left(\frac{r_0}{r_0-s}\right)$ is close to unity and by assuming that CHF conditions of the term $\{[\dot{m}_2/2\pi(r_0-s)](\Delta x_2/\Delta z)\}$ are negligible. This latter assumption will be justified subsequently. We then have

$$G_3(x_2-x_1) = \frac{q''_b}{h_{fg}}. \quad (5)$$

Further, we make use of the current view [25] that

$$q''_b = q''\frac{(h_l-h_{ld})}{(h_f-h_{ld})} \quad (6)$$

and then write in dimensionless form

$$\frac{q''}{h_{fg}G_3}\frac{(h_l-h_{ld})}{(h_f-h_{ld})} = (x_2-x_1). \quad (7)$$

From our basic postulates, the heat flux, q'', evaluated from equation (7), becomes the critical heat flux when x_2 corresponds to the critical void fraction.

The critical void fraction was determined by estimating the maximum void fraction at which separate bubbles could be maintained in the bubbly layer. Examination of a limited number of photographs of the bubbly layer [26, 27] indicated that the bubbles are approximately ellipsoidal with the ratio of long and short ellipse axis being about 3:1. It was therefore postulated that the maximum void fraction was obtained when the bubbly layer was filled with such bubbles which were just touching. An infinite array of such bubbles was found to correspond to a void fraction of 0.82. The value of x_2 was computed from this α with the assumption that vapor slip was negligible. This latter assumption is believed to be reasonable at the high mass flow rates to which this study was restricted ($G \geqslant 3.15\times10^6$ kg m^{-2} h^{-1}).

The fluid enthalpy at the detachment point was evaluated using Levy's model [25, 28]. The critical heat flux could then be evaluated for values of x_1 and h_1 corresponding to particular tests once an expression for G_3, the mass flow rate from core to bubbly layer, was developed.

4. TURBULENT TRANSPORT BETWEEN CORE AND BUBBLY LAYER

The evaluation of mass flow between the core and bubbly layer is based on an estimation of the magnitude of fluctuating radial velocity components at the bubbly layer–core interface. Several investigators have noted the effect of the presence of bubbles in increasing turbulence. Michiyoshi [29] makes the assumption that the eddy diffusivity of a two-phase bubbly mixture can be obtained as the product of the single phase eddy diffusivity at the given location in the tube and a multiplier based on liquid and vapor properties. We proceed similarly.

Laufer's [30] measurements of turbulent radial velocity fluctuations in round tubes are widely accepted. Recently, Lee and Durst [24] pointed out that the ratio $[\overline{(v')^2}^{1/2}/U_\tau]/(l_e/r_0)$ does not depend on Reynolds number and can be considered to be only a function of (r/r_0). As may be seen in Fig. 2, the relationship (dotted line)

$$[\overline{(v')^2}^{1/2}/U_\tau]/(l_e/r_0) = 2.9(r_0/y)^{0.4} \quad (8)$$

where $y = r_0-r$, is a good approximation of Durst's curve (solid line). With the assumption that the ratio of two-phase to single phase turbulent intensity is independent of radial position we have

$$\left(\frac{\overline{v'^2}^{1/2}}{U_\tau}\right) = 2.9F_1\left(\frac{r_0}{y}\right)^{0.4}\left(\frac{l_e}{r}\right). \quad (9)$$

By making use of generally accepted relationship stating

$$l_e = 0.4y \quad (10)$$

we have

$$\frac{\overline{v'^2}^{1/2}}{U_\tau} = 1.16F_1\left(\frac{y}{r}\right)^{0.6}. \quad (11)$$

From the definition of U_τ and the variation of f' with Reynolds number in the turbulent region, we obtain

$$U_\tau = \left(\frac{f'}{2}\right)^{1/2}\frac{G}{\bar{\rho}} = \left(\frac{0.046Re^{-0.2}}{2}\right)^{1/2}\frac{G}{\bar{\rho}} = (0.023)^{1/2}Re^{-0.1}\left(\frac{G}{\bar{\rho}}\right). \quad (12)$$

By use of the foregoing expression for U_τ in equation (11) we get

$$\frac{\overline{v'^2}^{1/2}}{G} = \frac{0.176}{\bar{\rho}}F_1Re^{-0.1}\left(\frac{y}{r_0}\right)^{0.6}. \quad (13)$$

In developing equation (13), we made the tacit assumption that the two-phase mixture could be treated as a homogeneous fluid. Frictional losses were then obtained as if the mixture were a homogeneous

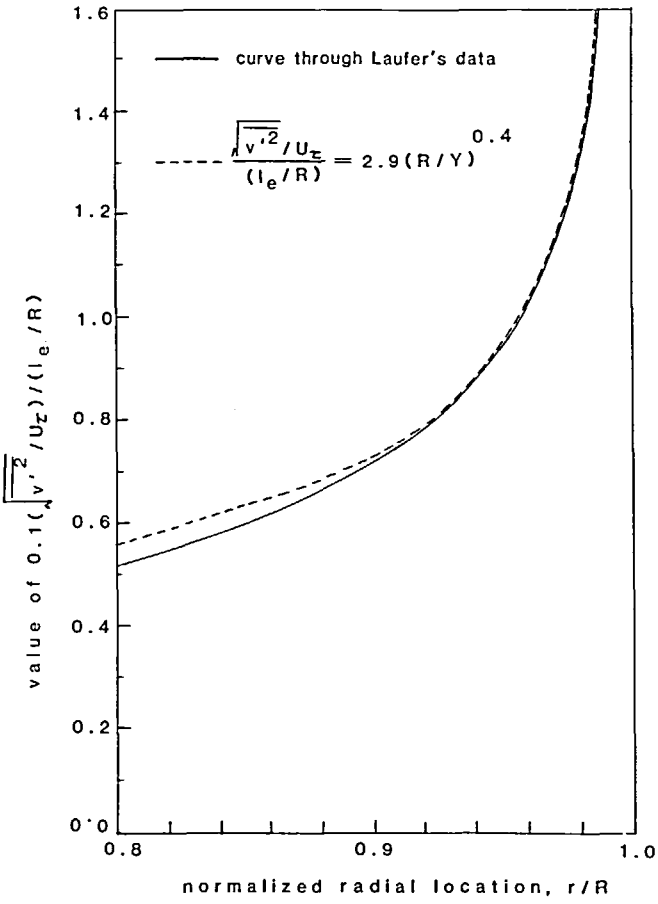

FIG. 2. Single phase radial velocity fluctuations as function of position.

fluid with an average fluid density, $\bar{\rho}$. This latter assumption is in general accord with observations of two-phase pressure drop at the high mass velocities to which the current development is restricted.

The assumptions made require that the turbulent interchange be evaluated at the core–bubbly layer interface. To determine the location of the bubbly layer–core interface, we rely on Lee and Durst's [24] postulate that the bubbly layer terminates when the eddy size is significantly larger than the bubble diameter, D_p. If we take the Prandtl mixing length as an index of eddy size and assume that the Prandtl mixing length in a two-phase mixture is $(F_2 l_e)$, then the turbulent intensity must be evaluated at a distance from the wall where

$$F_2 l_e = kD_p. \tag{14}$$

Hence, by using equation (10) we have that y_c, the distance from the wall at which the bubbly layer–core interface occurs, is

$$y_c = (kD_p)/(0.4\,F_2). \tag{15}$$

We determine the turbulent intensity at the core–bubbly layer interface by replacing y in equation (13) by y_c. This yields

$$\overline{v'^2}^{1/2}\left(\frac{\bar{\rho}}{G}\right) = 0.176\left(\frac{F_1}{F_2^{0.6}}\right)Re^{-0.1}\left(\frac{k}{0.4}\right)^{0.6}\left(\frac{D_p}{r_0}\right)^{0.6} = i_b. \tag{16}$$

To obtain the turbulent velocity fluctuations from the foregoing radial turbulent intensity at the interface, we assume that the turbulent velocity fluctuations are normally distributed. This is reasonable since they are produced by a large number of random effects. This assumption was also made by McKelvey [31] who successfully computed mass transfer rates via turbulent velocity fluctuations at an interface. Since the velocity fluctuation has a mean, $\bar{v}'$, of zero we have

$$f(v') = \frac{1}{(\sqrt{2\pi})\sigma_{v'}}\exp -\left[\frac{1}{2}\left(\frac{v'}{\sigma_{v'}}\right)^2\right]. \tag{17}$$

From any large sample of N experimental observations we would estimate $\sigma_{v'}^2$ from

$$\sigma_{v'}^2 \simeq \left(\frac{\sum_i^N (v')^2}{N}\right) - (\bar{v}')^2 = \frac{\sum_i^N (v')^2}{N} = \overline{v'^2}. \tag{18}$$

Hence

$$\sigma_{v'} = \overline{v'^2}^{1/2} \tag{19}$$

and we may evaluate $\sigma_{v'}$ from equation (16). That is,

$$\sigma_{v'} = (G/\bar{\rho})i_b. \tag{20}$$

Scriven [32] has shown how gross flow away from an interface can retard heat and mass transfer at that interface. The flow reduces the turbulent diffusion towards the interface as it prevents small size velocity fluctuations from reaching the wall. If we assume that the quantity of vapor generated in the bubbly layer which remains in the bubbly layer is small and essentially all the vapor generated flows into the core, then $v_{11} = q''_b/\rho_g h_y$ is the average velocity at which vapor is flowing away from the wall. Only those velocity fluctuations which are larger than v_{11}, and which are directed towards the heated wall, can penetrate to the interface. Quantitatively

$$G_3 = \bar{\rho}\int_{v_{11}}^{\infty}(v'-v_{11})f(v')\,dv. \tag{21}$$

Pei [36] shows that the integral can be expressed as

$$\int_{v''}^{\infty}(v'-v_{11})f(v')\,dv = \sigma_{v'}\left\{\frac{1}{(\sqrt{2\pi})}\exp-\left[\frac{1}{2}\left(\frac{v_{11}}{\sigma_{v'}}\right)^2\right] - \frac{1}{2}\left(\frac{v_{11}}{\sigma_{v'}}\right)\mathrm{erfc}\left(\frac{1}{\sqrt{2}}\frac{v_{11}}{\sigma_{v'}}\right)\right\} = \sigma'_{v'}\psi. \tag{22}$$

By combining equations (20)–(22) we have

$$G_3 = G\psi i_b. \tag{23}$$

The basic predictive equation [equation (7)] may now be rewritten in more convenient form,

$$\frac{q''}{h_{fg}G}\left(\frac{h_l-h_{ld}}{h_f-h_{ld}}\right) = (x_2-x_1)\psi i_b. \tag{24}$$

To proceed further it is necessary to develop an expression for $(F_1/F_2^{0.6})$ in order to evaluate i_b. It is to be expected that F_1, which represents the effect of bubble motion on turbulent intensity will be the most significant factor. Indeed, the factor F_2, representing the effect of bubble motion on mixing length, may be unity. Correlations of the effect of bubble motion on turbulent intensity are not available although several investigators [33–35] have proposed expressions for the effect of bubble motion on the eddy diffusivity. Serizawa *et al.* [35] correlated their measurements of the ratio of two-phase to single-phase eddy diffusivity in the turbulent core in terms of the Lockhart–Martinelli modulus, X, which is itself a function of quality, gas–liquid density ratio and gas–liquid viscosity ratio. In the present case, a preliminary examination of the data indicated that the ratio (ρ_g/ρ_l) was the dominant factor the turbulent intensity enhancement. For simplicity, the ratio (F_1/F_2) was assumed to be in the form

$$(F_1/F_2^{0.6}) = \left[1+a\left(\frac{\rho_l-\rho_g}{\rho_g}\right)\right] \tag{25a}$$

and hence

$$i_b = 0.462Re^{-0.1}(k)^{0.6}\left(\frac{D_p}{D}\right)^{0.6}\left[1+a\left(\frac{\rho_l-\rho_g}{\rho_g}\right)\right]. \tag{25b}$$

Note that at the critical pressure the ratio $F_1/F_2^{0.6}$ would equal unity. The values of both a and k were determined by an empirical fit of experimental CHF data.

5. CALCULATION OF BUBBLE DIAMETER, BUBBLE DETACHMENT POINT, SUBCOOLED QUALITY AND CHF

Final evaluation of the critical heat flux requires values for the average bubble diameter and average quality and density. The bubble diameter was evaluated using Levy's [28] model which balances buoyancy and drag forces against surface tension. At the high velocities of current interest, buoyant forces are negligible and the bubble diameter may be written as [36]

$$D_p = 0.015\left(\frac{8\bar{\rho}g_c\sigma D_h}{f'G^2}\right)^{1/2}. \tag{26}$$

Over the range of conditions examined, bubble diameters ranged from 0.001 to 0.005 cm.

Since most of the low quality critical heat flux data is in the subcooled boiling range, an appropriate model for subcooled quality is required. Lahey's [37] subcooled boiling model was chosen as best representing the current state of the art. Lahey's approach, as well as the estimation of q''_b, requires the determination of the enthalpy at which bubble detachment begins. Recent tests by Edelman and Elias [38] indicate that both the Saha and Zuber [39] and Levy [28] models are adequate for this purpose. The Levy [28] model was chosen on the basis that it had a phenomenological base.

An iterative procedure is required for computing the predicted value of q''_{DNB} since the function ψ, on the RHS of the predictive equation [equation (24)] depends on q''. A value for q'' is assumed and Levy's [28] model is used to calculate the location, z_d, and the enthalpy h_{ld}, at the bubble departure point. An iterative approach is then used to calculate x_{avg} and h_l at the z_{CHF}, which is at the end of the tube (critical heat flux location for uniformly heated tubes). The values of i_b and ψ are then computed. By assuming $\alpha_2 = 0.82$ at z_{CHF}, x_2 is evaluated at z_{CHF} thus allowing x_1 and ρ_1 to be determined at this evaluation.

After rearranging the predictive equation so that it is written in the form

$$q''_{DNB} = h_{fg}G(x_2-x_1)i_b\psi\left(\frac{h_f-h_{ld}}{h_l-h_{ld}}\right), \tag{27}$$

the previously determined parameters are used to determine the value of the RHS of equation (27). If the assumed heat flux equals the value predicted by the RHS within a preassigned tolerance, the procedure is

terminated. If not, another value of q'' is assumed and the process repeated. The equations used in the calculation procedure are summarized in Appendix 1.

6. COMPARISON OF PROPOSED PREDICTIVE PROCEDURE WITH UNIFORM HEAT FLUX WATER DATA

The proposed predictive procedure was compared to slightly more than 1500 data points obtained with water in uniformly heated round tubes. The data points were obtained from refs. [40–53]. Only runs in which the entering fluid was below the saturation enthalpy and in which the exit fluid was subcooled or at a low quality were considered. The range of parameters considered were:

P 20–205 bars,
G $3.5 \times 10^6 - 49 \times 10^6$ kg m^{-2} h^{-1},
L 0.35–360 cm,
D 0.115–3.75 cm,
$\alpha_{CHF} \leqslant 0.6$.

A high minimum mass velocity was selected so as not to depart greatly from the homogeneous flow assumption. The maximum α examined was limited to 0.6 to assure that annular flow would not be encountered. Tube diameters examined were limited to what was believed the range of interest. Pressure and test section length ranges were set by the range of usable data available in the reference sources chosen.

The first task was to determine the appropriate values of a and k to be used in equation (25). It was initially assumed that a constant value of a would be satisfactory and a trial and error procedure was used to locate the best values of a and k. In order to determine the most satisfactory values of these parameters for round tube water data, the quantity R was defined as

$$R = \frac{\text{predicted critical heat flux}}{\text{experimentally observed critical heat flux}}. \quad (28)$$

The values of a and k were varied so as to obtain a $\mu(R)$ of ~ 1.0 while minimizing $\sigma(R)$. The best constant value of a was found to be 0.135 and k to be 2.28. However, although a reasonable correlation was obtained, a comparison of predictions and observations showed that the degree of agreement depended on the flow rate. This is not surprising since it is to be expected that the relative contribution of bubble motion to the total turbulence level will decrease as the mass velocity is increased. A trial and error procedure was again used to locate the exponent and multiplier for G which minimized the $\sigma(R)$ value maintaining $\mu(R) \simeq 1.0$. It was found that

$$i_b = (GD/\mu_{avg})^{-0.1}(D_p/D)^{0.6}[1 + a(\rho_l - \rho_g)/\rho_g]$$

$$a = 0.135, \quad G \leqslant 9.7 \times 10^6 \text{ kg h}^{-1} \text{ m}^{-2}$$

$$a = 0.135(G/9.7 \times 10^6)^{-0.3}, \quad (29)$$

provided the best fit. The value of k changed slightly to 2.4.

To evaluate the accuracy of the final correlation the values of $\sigma(R)$ and $\mu(R)$ for the proposed correlation were compared with $\sigma(R)$ and $\mu(R)$ for two well known empirical correlations. The so called W-3 correlation due to Tong [54] was selected since it is generally regarded as providing one of the best representations of round tube data within its range. The CISE correlation due to Bertolleti *et al.* [56] was chosen because the wide parameter range over which it is applicable and the fact that it has been found useful in rod bundles. The upper half of Table 1 compares the three correlations for only those round tube uniformily heated test section data points falling within the range of parameters over which the W-3 correlation is valid. It may be seen that the present correlation is considerably more accurate than the CISE correlation and about as accurate as the W-3 correlation. It should be noted that the W-3 correlation requires 17 empirical constants while the present correlation requires only three.

The lower half of Table 1 compares the three sets of predictions for all of the uniformly heated round tube test section data points examined. Although the accuracy of the present approach is lower than it was within the limited parameter range previously examined, the present correlation is clearly far superior to the others. The accuracy of the W-3 correlation

Table 1. Comparison of predictions and experimental data—water in uniformly heated round tube

Prediction	Number of data points	$\mu(R)$	$\sigma(R)$
W-3 correlation	406 (W-3 range)	0.989	0.059
CISE correlation	406 (W-3 range)	1.012	0.118
Present correlation	406 (W-3 range)	0.994	0.065
W-3 correlation	1516	1.131	0.570
CISE correlation	1516	0.946	0.178
Present correlation	1516	0.9995	0.099

deteriorates very badly once its allowable parameter range is exceeded.

Figure 3 provides a visual comparison of predicted and observed critical heat fluxes for uniformly heated test sections using water. In view of the difficulty of showing 1500 points on a single plot, only one out of each ten points examined is plotted. A random number generator was used to assure that points shown were selected in a random manner.

7. SENSITIVITY OF PREDICTIONS TO ASSUMPTIONS MADE

In deriving the proposed model, several assumptions were made which require further justification. For example, we assumed that in equation (4) the ratio $[r_0/(r_0-s)]$ could be taken as unity. Since the value of k has been determined and the bubbly layer thickness can be estimated. Over 200 runs were randomly selected from among those examined and values of s at the CHF point determined. Revised critical heat flux prediction were calculated by incorporating the ratio in the predictive equation. In all cases the variation in CHF prediction was less than 0.7% and the assumption made is therefore justified.

In simplifying the mass balance of equation (4), it was also assumed that the term

$$\frac{\dot{m}_2}{2\pi(r_0-s)}\left(\frac{\Delta x_2}{\Delta z}\right)$$

could be neglected. This assumption was initially evaluated by writing a computer program which calculated the value of $\dot{m}_2$ and x_2 in a stepwise fashion along the channel. The energy and mass balances used were the same as those for the CHF location except that x_2 was computed from the value at the previous length step and the change in x_2 in the length step examined. In this calculation the conservative assumption (conservative in that it over estimated the effect of omitted term) was made that the velocity in the bubbly layer equaled the linear velocity in the core. For the several cases examined, the values of

$$\frac{\dot{m}_2}{2\pi(r_0-s)}\left(\frac{\Delta x_2}{\Delta z}\right)$$

were found to be negligible. However, the procedure was somewhat lengthy and its application to a large number of cases seemed cumbersome. An approximate expression for the value of this omitted term was found

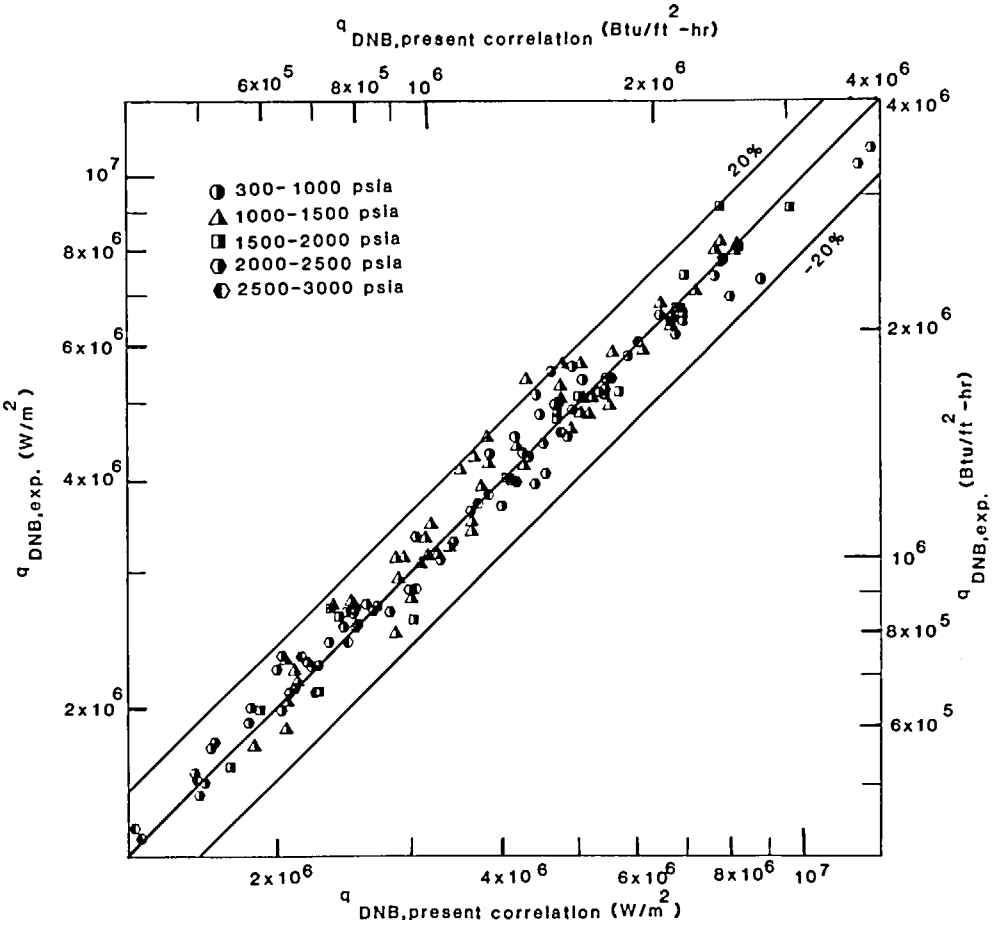

FIG. 3. Comparison of predicted and observed critical heat fluxes in uniformly heated round tube sections using water as coolant.

to be

$$\frac{KA_2V_2}{2\pi(r_0-s)G_3}\left(\frac{\Delta x_2}{\Delta z}\right)^2-\left[1+\frac{1}{2\pi(r_0-s)G_3}\right.$$
$$\times\left(A_2\rho_2\frac{\Delta V_{avg}}{\Delta z}\right)-\frac{KA_2V_2}{\dot m_1}(x_2-x_1)+\left.\frac{\dot m_2}{\dot m_1}\right]\left(\frac{\Delta x_2}{\Delta z}\right)$$
$$+\left[\left(\frac{\dot m_t}{\dot m_1}\right)\frac{\Delta x_{avg}}{\Delta z}-\frac{A_2\rho_2}{\dot m_1}(x_2-x_1)\frac{\Delta\bar V}{\Delta z}\right]=0 \qquad (30)$$

where

$$K=\mathrm{d}\rho_2/\mathrm{d}x.$$

With the conservative assumption that the bubbly layer velocity equals the velocity in the core, the results obtained from equation (30), when the root corresponding to $[-b-(b^2-4ac)^{1/2}/2a]$ was used, compared well to the results of the stepwise calculation. Equation (30) was then used to evaluate the effect of the omitted term in 700 experimental runs. The error produced in the CHF was almost always less than 1%.

The effect of changes in the assumption that the bubbly layer void fraction was 0.82 was examined. When this value was varied from 0.79 to 0.85 and the predictive equation adjusted so that $\mu(R)\simeq 1.0$, very little change in $\sigma(R)$ was seen. However, the lowest $\sigma(R)$ coincided with $\alpha_2=0.82$.

Since there is not general agreement on whether the approach of Saha and Zuber [39] or Levy [28] provides the best estimate of the enthalpy at bubble detachment, both approaches were tried. The value of $\mu(R)$ was closer to 1.0 and $\sigma(R)$ lower with the Levy [28] model than for the Saha–Zuber [39] model.

8. APPLICATION OF PREDICTION PROCEDURE TO NON-UNIFORMLY HEATED ROUND TUBES

At high exit qualities (annular flow regime) there is agreement that the location of dryout is determined primarily by the total heat input and test section length rather than the local heat flux. Thus, Bertoletti *et al.* [56] showed that data from rods with a non-uniform axial flux shapes could be related to data from uniformly heated tubes by using the "saturated length" concept. The saturated length is defined as the distance from the position of zero thermodynamic quality to the point in question. Non-uniform and uniform heat flux data, at the same mass velocity and pressure, have been shown to fall on a single curve of q_s'' vs length when q_s'' is defined as the heat flux averaged over the saturated length.

At low exit qualities there has been general agreement that the CHF phenomenon is primarily a local condition. However, in order to relate data from non-uniformly heated rods to empirical correlations developed for uniformly heated rods, a correction factor is commonly employed. The usual approach is due to Tong [9] who extended the *W*-3 correlation to non-uniformly heated channels by writing.

$$q''_{DNB,NU}=q''_{DNB,EU}/F \qquad (31)$$

where

$q''_{DNB,NU}$ = DNB heat flux for the non-uniformly heated channel,

$q''_{DNB,EU}$ = equivalent uniform DNB flux from *W*-3 correlation for uniform heat flux DNB predictions,

$$F=\frac{C}{q''_{local}[1-\exp(-Cl_{DNB,EU})]}\times\int_0^{l_{DNB,N}}q''(z)\exp[-C(l_{DNB,N}-z)\,\mathrm{d}z, \qquad (32)$$

$$C=0.15\frac{(1-X_{DNB})^{4.31}}{(G/10^6)^{0.478}}[\text{in.}^{-1}], \qquad (33)$$

$l_{DNB,EU}$ = axial location at which DNB occurs for uniform heat flux [in.],

$l_{DNB,N}$ = axial location at which DNB occurs for non-uniform heat flux [in.],

x_{DNB} = quality at DNB location under non-uniform heat flux conditions.

Tong has argued that there is a theoretical justification for this approach since upstream heat flux distributions affect the bubbly layer at the DNB position. Wilson *et al.* [57] have used the same approach with essentially the same expression for F with their own empirical critical heat flux correlation. However, in adapting still another uniform heat flux correlation to some non-uniformly heated rod-bundle data, one investigator has found that no correction factor was required [58].

If the present predictive approach is valid, it should be applicable to non-uniformly heated round tube CHF data which fall within the allowed parameter range. The data of Bennett *et al.* [59] and Swenson *et al.* [60] for round tubes with non-uniform axial heating were taken as typical of the available data of this type. These data were compared to predictions obtained from the presently proposed approach (using the same empirical coefficients found for uniformly heated tubes) and the *W*-3 correlation [54] with the F factor correction. All of these data which fell within the range of the present approach were also within the *W*-3 range.

To apply the present correlation to non-uniformly heated tubes, a value of q''_{max} is assumed and the local heat flux determined as a function of length. The values of x_1, ρ_1, h_l, $(h_l-h_{ld})/(h_f-h_{ld})$, i_b, ψ are determined as a function of length using the appropriate local heat fluxes. By using x_2 corresponding to $\alpha=0.82$ for the axial locations downstream of the location of q''_{max}, the predicted critical heat flux is determined from equation (2). The DNB ratio (DNB ratio = predicted critical heat flux/local heat flux) is then determined as a function of length and the minimum value noted. If the minimum DNB ratio does not equal one, then the value of q''_{max} is adjusted until the value is found at which the minimum DNB ratio is one. The value of q''_{max} so obtained is then compared with the q''_{max} actually observed at CHF conditions. Computations of the *W*-3 predictions proceeded similarly with q''_{max} being

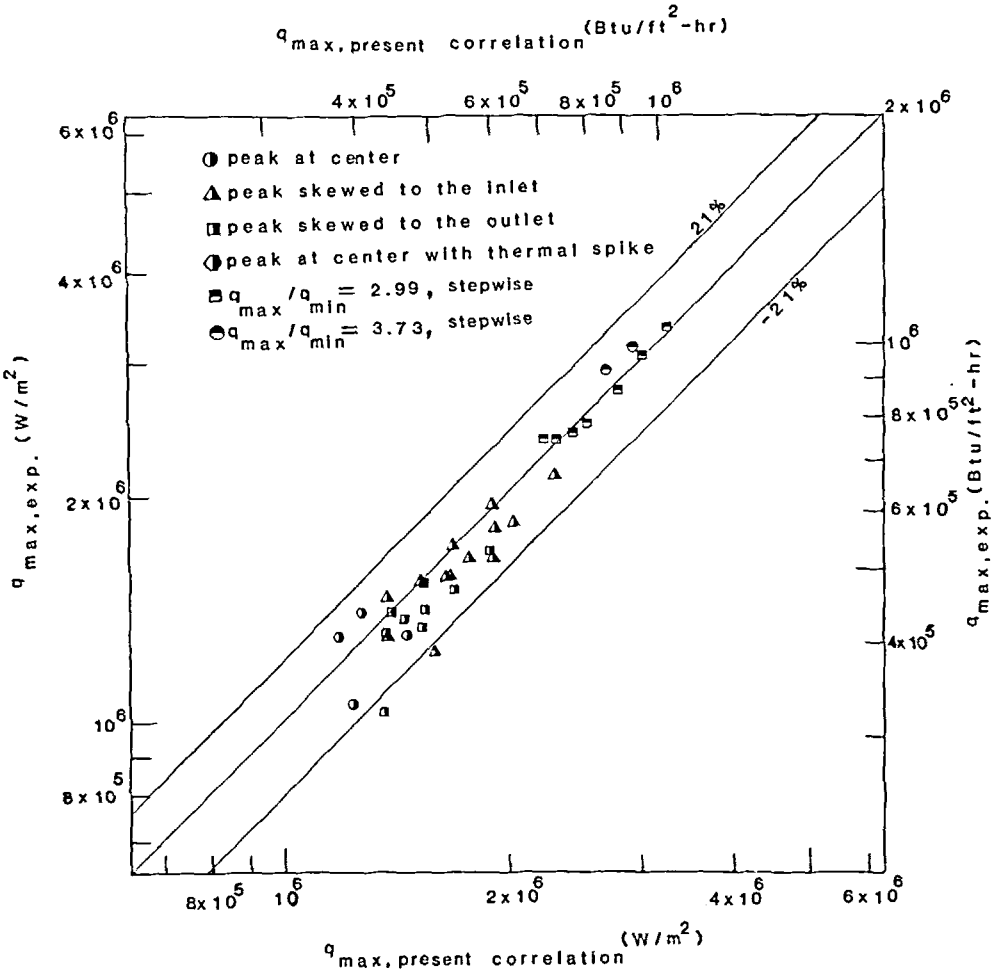

FIG. 4. Comparison of predicted and observed critical heat flux; non-uniformly heated test sections (water at 68 and 136 bar).

adjusted until a minimum DNB ratio of one was obtained.

The available data included experiments with 6 different flux distributions and at pressures of 68 and 136 bar. A visual comparison of the predictions and observations are shown in Fig. 4. It may be seen that observations and predictions compare well. The statistical evaluation of these results and the *W*-3 predictions using the *F* factor (Table 2) indicate that the present approach is only slightly less precise than the *W*-3 correlation. The good agreement obtained with the present predictive approach would appear to sustain the view that, at low qualities, CHF is a local phenomenon.

Table 2. Comparison of axially non-uniform heat flux water data with predictions

Correlation	Number of data points	$\mu(R)$	$\sigma(R)$
W-3 (with *F* factor)	35	1.061	0.083
Present prediction	35	1.046	0.104

9. PREDICTIONS OF CHF FOR FLUIDS OTHER THAN WATER

If the present predictive approach is soundly based, it should be capable of providing reasonable CHF predictions for fluids other than water without any change in the empirical constants. The proposed predictive method was therefore compared to experimental data in the literature which were obtained with refrigerant 11 [61], refrigerant 113 [62], liquid nitrogen [63] and anhydrous ammonia [64]. All data were obtained with uniformly heated round tubes.

The results of this comparison are shown graphically in Fig. 5 and the statistical comparison is given in Table 3. Although the results are not as accurate as those obtained with water, the comparison is still quite good considering the wide range in experimentally observed critical heat fluxes.

10. CONCLUSION

A phenomenologically based prediction of critical heat flux conditions, during flow boiling at high

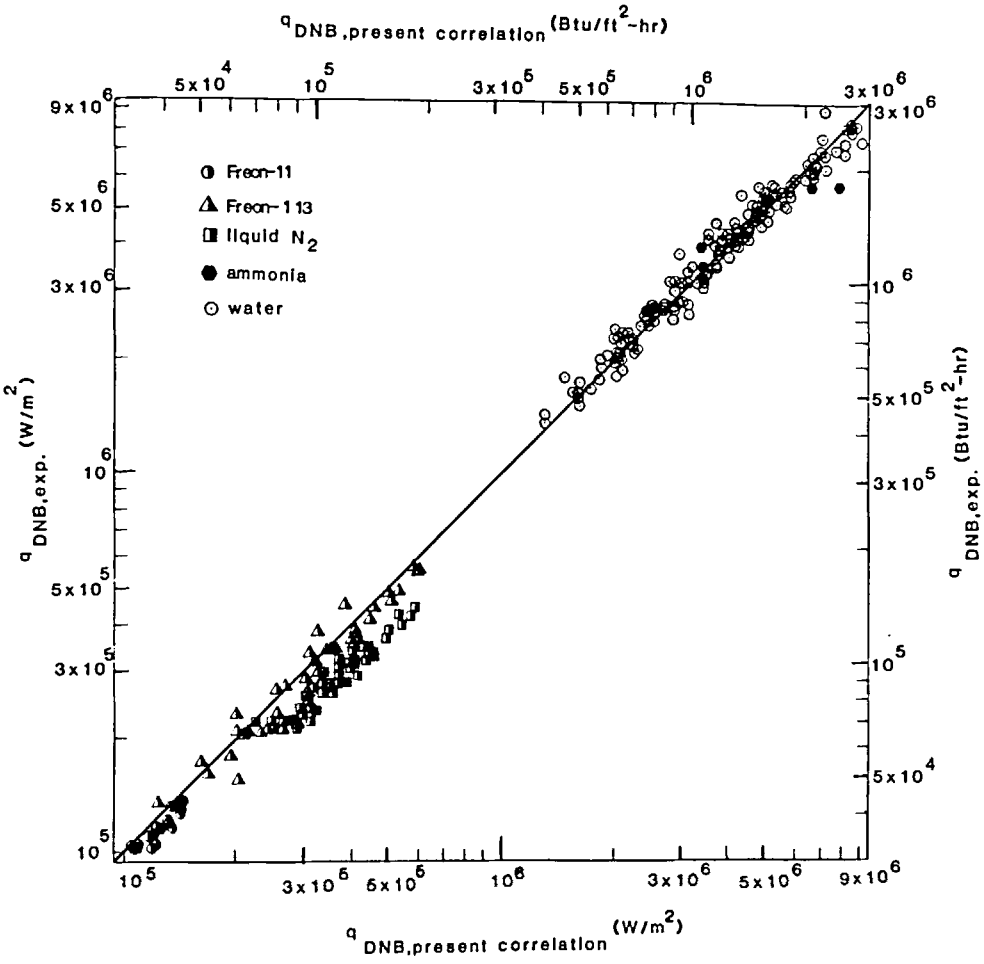

FIG. 5. Comparison of predicted and observed critical heat fluxes for several fluids (uniformly heated round tubes).

velocities and low qualities has been developed. With adjustment of only three empirical coefficients, the predictions of uniformly heated round tube data are nearly as accurate as those obtained from the W-3 correlation [52] in the narrow W-3 range. The predictive method can, however, be used well outside the range of W-3 correlation with little loss in accuracy. The present approach was considerably more accurate than either the W-3 [54] or CISE [55] correlations over the expanded range.

Table 3. Comparison of uniformly heated round tube data for several fluids with predictions of present procedure

Fluid	Number of data points	$\mu(R)$	$\sigma(R)$
Freon 11	20	1.071	0.048
Freon 113	40	1.054	0.094
Liquid N_2	50	1.302	0.098
Anhydrous ammonia	7	1.168	0.285
All non-water data	117	1.169	0.159
Water	1516	0.9995	0.099

The present approach is capable of accurately predicting critical heat fluxes in axially non-uniformly heated round tubes. No distribution correction factors need be applied. This would appear to confirm the supposition that, at low qualities, the critical heat flux is governed by local conditions. The requirement for the use of distribution correction factors with some empirical correlations may simply be due to the empirical manner in which subcooling effects are computed.

The ability of the present method to provide reasonable predictions with fluids other than water is believed to be a further validation of the approach. No scaling factors are required. Particularly good accuracy was obtained with refrigerants 11 and 113 which are often used to evaluate the general effect of design changes on critical heat fluxes. The present predictive method should enhance such applications.

Further development of the present correlation would be desirable. It would be useful to consider the effect of vapor slip so that the lower mass velocity limit could be decreased. In addition, the simple dependence of the two-phase turbulent intensity multiplier on G

alone needs to be re-examined. Replacing G by a function of Reynolds number was tried without satisfactory results.

Much of the current need for CHF prediction is concerned with CHF behavior in rod bundles. Although the applicability of the present approach to rod bundle data has not been examined, it is believed that this would be a worthwhile study. Leung and Henry [65] have shown that the CISE [55] round tube correlation can be used for prediction of CHF in rod bundles if appropriate local conditions are used with the correlation. If we let $R = (q''_{CHF}$, present approach)/(q_{CHF}, CISE), we find $\mu(R) = 0.98$ and $\sigma(R) = 0.12$, for 150 randomly selected data points within the W-3 range. The agreement between the CISE correlation and the present approach, and the ability of the CISE correlation to predict rod bundle data, implies that the present approach may be useful for predicting rod bundle behavior.

REFERENCES

1. S. Levy, J. M. Healzer and D. Abdollahian, Prediction of critical heat flux for annular flow in vertical pipes, EPRI Report NP-1619 Electric Power Research Inst., Palo Alto, California (1980).
2. E. J. Thorgerson, D. H. Knoebel, and J. H. Gibbons, A model to predict convective subcooled critical heat flux, *Trans. Am. Soc. Mech. Engrs*, Series C, *J. Heat Transfer* **96**, 79–82 (1974).
3. A. E. Bergles, Burnout in boiling heat transfer. Part II: Subcooled and low-quality forced-convection systems, *Nuclear Safety* **18**, 154–167 (1977).
4. S. S. Kutadeladze and A. I. Leont'ev, Some applications of the asymptotic theory of the turbulent boundary layer, *Proc. 3rd Int. Heat Transfer Conf.*, Chicago, Vol. 3 (1966).
5. Y. P. Chang, Some possible critical conditions in nuclear boiling, *Trans. Am. Soc. Mech. Engrs*, Series C, *J. Heat Transfer* **85**, 89–100 (1973).
6. W. R. Gambill, Generalized prediction of burnout heat flux for flowing, subcooled, wetting liquids, *A.I.Ch.E. Symp. Ser.* **59**, 71–87 (1963).
7. S. Levy, Prediction of the critical heat flux in forced convection flow, USAEC Report GEAP-3961, General Electric Company (1962).
8. M. P. Fiori and A. E. Bergles, Model of CHF in subcooled flow boiling, Paper b 6.3, *Heat Transfer 1970*, Vol. 6, *Proc. 4th Int. Heat Transfer Conf.*, Versailles (1970).
9. L. S. Tong, H. B. Currin, P. S. Larsen and D. G. Smith, Influence of axially non-uniform heat flux on DNB, *A.I.Ch.E. Symp. Ser.* **64**, 35 (1965).
10. L. S. Tong, Boundary layer analysis of the flow boiling crisis, *Int. J. Heat Mass Transfer* **11**, 1208–1215 (1968).
11. W. T. Hancox and W. B. Nicoll, On the dependence of the flow-boiling heat transfer crisis on local near-wall conditions, ASME Paper 73-HT-38 (1973).
12. W. Hebel and W. Detavernier, Critical heat transfer rate to flowing cooling water, *Kerntechnik* **19**, 228–232 (1977).
13. W. Hebel, W. Detavernier and M. Decreton, A contribution to the hydrodynamics of boiling crisis in a forced flow of water, *Nucl. Engng Des.* **64**, 433–445 (1981).
14. I. P. Smogalev, Calculation of critical heat fluxes with flow of subcooled water at low velocity, *Thermal Engng* **28**, 208–213 (1981).
15. O. Kampfenkel, A theory of similarity of the departure from Nucleate boiling in forced convection flow, *Atom Kernenergie* **15**, 205–210 (1970).
16. L. I. Glushehenko, Correlation of experimental data on critical heat fluxes in subcooled boiling, *Heat Transfer—Soviet Res.* **2**, 139–163 (1970).
17. A. P. Ornatskii, L. F. Glushenko and E. M. Maevskii, Critical heat flux in steam generating tubes in the region of low subcooling and steam content, *Thermal Engng* **18**, 106–109 (1971).
18. Y. Katto, A generalized correlation of critical heat flux for the forced convection boiling in vertical uniformly heated round tubes, *Int. J. Heat Mass Transfer* **21**, 1527–1542 (1978).
19. Y. Katto, A generalized correlation of critical heat flux for the forced convection boiling in vertical uniformly heated round tubes—A supplementary report, *Int. J. Heat Mass Transfer* **22**, 783–794 (1978).
20. F. C. Gunther, Photographic studies of surface boiling heat transfer to water with forced convection, *Trans. ASME* **73**, 115–121 (1951).
21. L. S. Tong, A. A. Bishop and L. E. Efferding, A photographic study of subcooling boiling flow and DNB of Freon-113 in a vertical channel, ASME Paper 66-WA/HT-39 (1966).
22. L. M. Jiji and J. A. Clark, Bubble boundary layer and temperature profiles for forced convection boiling in channel flow, *Trans. Am. Soc. Mech. Engrs*, Series C, *J. Heat Transfer* **86**, 50–61 (1964).
23. G. J. Kirby, R. Stanforth and J. H. Kinnely, A visual study of forced convection boiling—Part I: Results for a flat vertical heater, UKAEE Report No. AEEW-R-281 (1965).
24. S. L. Lee and F. Durst, On the motions of particles in turbulent flow, U.S. Nuclear Regulatory Commission Report NUREG/CR-1556 (1980).
25. R. T. Lahey and F. Moody, *The Thermal Hydraulics of a Boiling Water Reactor*, pp. 214–220. American Nuclear Society, La Grange Park, Illinois (1977).
26. L. S. Tong, *Boiling Heat Transfer and Two-Phase Flow*, p. 141. John Wiley, New York (1965).
27. M. Cumo, G. E. Farello, G. Ferrari, M. Montanari and P. Nozzi, On two-phase thermal boundary layer along heated walls, Report to the National ATI Annual Meeting, Cagliari (1975).
28. S. Levy, Forced convection subcooled boiling—Prediction of vapor volumetric fraction, GEAP-5157, General Electric Company (1966).
29. I. Michiyoshi, Two-phase, two-component heat transfer, Keynote Paper, 6th Int. Heat Transfer Conf., Toronto (1978).
30. J. Laufer, The structure of turbulence in fully developed pipe flow, NACA Technical Note No. 2954 (1953).
31. K. N. McKelvey, Turbulent scalar transfer at high diffusivity ratios, PhD thesis, Ohio State University, Columbus, Ohio (1967).
32. L. E. Scriven, Penetration theory modeling, *Chem. Engng Educ.* **3**, 94–102 (1969).
33. D. A. Drew and R. T. Lahey, Jr., A mixing length model for fully developed turbulent two-phase flow, *Trans. ANS* **35**, 626 (1980).
34. Y. Sato and M. Sadatom, Momentum and heat transfer in two-phase bubble flow—I, *Int. J. Multiphase Flow* **7**, 167–177, (1981).
35. A. Serizawa, I. Kataoka and I. Michyoshi, Turbulence structure of air–water bubbly flow, *Int. J. Multiphase Flow* **2**, 247–260 (1975).
36. B. S. Pei, Prediction of critical heat flux in flow boiling at low qualities, PhD Thesis, University of Cincinnati, Cincinnati, Ohio (1981).
37. R. T. Lahey, Jr. and F. Moody, *The Thermal Hydraulics of a Boiling Water Nuclear Reactor*, Ch. 5, p. 173. American Nuclear Society, La Grange Park, Illinois (1977).
38. Z. Edelman and E. Elias, Void fraction distribution in low flow rate subcooled boiling, *Nucl. Engng Des.* **66**, 375–380 (1981).

39. P. Saha and N. Zuber, Point of net vapor generation and vapor void fraction in subcooled boiling, *Proc. 5th Int. Heat Transfer Conf.*, Vol. 4 (1974).
40. R. A. De Bortoli *et al.*, Forced convection heat transfer burnout studies for water in rectangular channels and round tubes at pressures above 500 psia, WAPD-188 (1958).
41. K. M. Becker *et al.*, Measurement of burnout conditions for flow of boiling water in vertical round ducts (Parts 1 and 2), Aktiebolaget Atomenergie, Sweden, Report A.E. 87 (1962) and A.E. 114 (1963).
42. D. H. Lee and J. D. Obertelli, An experimental investigation of forced convection burnout in high pressure water, Part 1, Round tubes with uniform flux distribution, UKAEA Rep. No. AEEW-R213 (1963).
43. B. Thompson and R. Macbeth, Boiling water heat transfer burnout in uniformly heated round tubes—A compilation of world data with accurate correlations, UKAEA Rep. No. AEEEW-R356 (1964).
44. D. H. Lee and D. J. Morris, Burnout and two-phase pressure drop for water at 1000 psia in round tubes with uniform and non-uniform heat flux distribution, UKAEA Rep. No. AEEW-R355 (1964).
45. R. R. Hood and L. Isakoff, Heavy water moderated power reactors progress report for June 1962, USAEC Report D.P. 755 (1962).
46. H. Firstenberg *et al.*, Compilation of experimental forced-convection quality burnout data with calculated Reynolds number, USAEC Report NDA-2131-16 (1960).
47. R. J. Weatherhead, Heat transfer flow instability and critical heat flux in a small tube at 200 psia, USAEC Report ANL 6715 (1963).
48. R. J. Weatherhead, Nucleate boiling characteristics and the critical heat flux occurrence in sub-cooled axial flow water systems, USAEC Report ANL 6675 (1963).
49. B. Matzner, Basic experimental studies of boiling fluid flow and heat transfer at elevated pressures, USAEC Report TID 18978 (1962).
50. E. D. Waters, J. K. Anderson, W. L. Thorne and J. M. Batch, Experimental observations of upstream boiling burnout, Paper presented at the 6th National Heat Transfer Conference, Boston, August 1963, A.I.Ch.E. Reprint No. 7; see also USAE Report, HW73902 (Rev.) (1963).
51. J. Griffel and C. F. Bonilla, Forced convection boiling burnout for water in uniformly heated tubular test sections, *Nucl. Struct. Engng* **2**, 1 (1965).
52. D. H. Lee and J. D. Obertilli, An experimental investigation of forced convection boiling in high pressure water, Part III, UKAEA Rep. No. AEEW-R355 (1965).
53. V. Y. Doroshchuk and F. P. Fried, Critical heat flux for water flowing in tubes, *Problems of Heat Transfer and Hydraulics of Two-Phase Media* (edited by S. S. Kutadeladze), Chap. 4. Pergamon Press, Oxford (1969).
54. L. S. Tong, Prediction of departure from nuclear boiling for an axially non-uniform heat flux distribution, *J. Nucl. Energy* **6**, 21–27 (1967).
55. G. P. Gaspari, C. Lombardi, G. Peterlongo, M. Silvestri and F. A. Tacconi, Heat transfer crisis with steam–water mixtures, *Energia Nucleare* **12**, 121–133 (1965).
56. S. Bertoletti, G. P. Gaspari, C. Lombardi, G. Peterlongo and F. A. Tacconi, A generalized correlation for predicting the heat transfer crisis with steam–water mixture, *Energia Nucleare* **11**, 10–14 (1964).
57. R. H. Wilson, L. J. Stanek, J. S. Gellerstadt, and R. A. Lee, Critical heat flux in non-uniformly heat rod bundles, *Two-Phase Flow and Heat Transfer in Rod Bundles* (edited by V. E. Schrock). ASME, New York (1969).
58. J. Handshue, Yankee Atomic Electric Corp., Framingham, Mass., personal communication (1981).
59. A. W. Bennett, G. F. Hewitt, H. A. Kearsey, R. K. F. Keeys and D. J. Pulling, Studies of burnout in boiling heat transfer to water in round tubes with non-uniform heating, *Trans. Instn Chem. Engrs, London* **45**, 319–330 (1967).
60. H. S. Swenson, J. R. Carver and C. R. Kakarala, The influence of axial heat flux distribution on the departure from nucleate boiling in a water cooled tube, ASME Paper 62-WA-2978 (1962).
61. J. C. Leung, Transient critical heat flux and blowdown heat-transfer studies, Nuclear Regulatory Commission Report, NUREG CR-1559 (ANL-80-53) (1980).
62. R. D. Coffield, Jr., W. M. Rohrer, Jr. and L. S. Tong, A subcooled DNB investigation of Freon 113 and its similarity to subcooled water DNB Data, *Nucl. Engng Des.* **11**, 143–153 (1969).
63. S. S. Papell, R. J. Simoneau and D. D. Brown, Buoyancy effects on critical heat flux of forced convective boiling in vertical flow, NASA Report, TN D-3672, Washington, D.C. (1966).
64. D. R. Bartz, Cal. Inst. Tech. Report, JP (Memo-NO. 20-137), Pasadena (1956).
65. J. Leung and R. E. Henry, Prediction of CHF in rod bundles using a round tube correlation, *Trans. ANS* **33**, 963–964 (1979).

APPENDIX 1

CHF CALCULATION PROCEDURE

$$\left(\frac{q''}{h_{fg}G}\right)\frac{(h_l-h_{ld})}{(h_f-h_{ld})}\bigg|_{z_{CHF}} = (x_2-x_1)\bigg|_{z_{CHF}} \psi i_b. \qquad \text{(A1)}$$

Assume value for q''

Calculation of h_{ld}

$$y_b^+ = 0.10\frac{(\sigma g_c D_h \rho_f)^{1/2}}{\mu_f},$$

$$\text{if} \quad 0 \leqslant y_b^+ \leqslant 5.0; \; h_f - h_{ld} = C_{pl}\frac{q''}{H_{1\phi}} - \frac{q''}{G\left(\frac{f}{8}\right)^{1/2}} Pr y_b^+$$

$$\text{if} \quad 5.0 \leqslant y_b^+ \leqslant 30.0; \; h_f - h_{ld} = C_{pl}\frac{q''}{H_{1\phi}} - 5.0\frac{q''}{G\left(\frac{f}{8}\right)^{1/2}} \times \{Pr + \ln[1 + Pr(y_b^+/5.0 - 1.0)]\}$$

$$\text{if} \quad y_b^+ \geqslant 30.0; \; h_f - h_{ld} = C_{pl}\frac{q_t''}{H_{1\phi}} - 5.0\frac{q_t}{G\left(\frac{f}{8}\right)^{1/2}} \times \{[Pr + \ln(1.0 + 5.0Pr) + 0.5\ln(y_b^+/30.0)]\}$$

where

$$Nu = 0.023 Re^{0.8} Pr^{0.4} = \frac{H_{1\phi} D}{k_l},$$

$$Re = GD/\mu_l, \quad Pr = c_p \mu_l / k_l.$$

Iterative calculation of x_{avg} and h_l

$$x_{avg} = \frac{1}{GAh_{fg}}\left\{\int_{z_d}^{z_{CHF}} \frac{p_H q_b''\, dz}{(1+\varepsilon)} - \int_{z_d}^{z_{CHF}} p_H q_{cond}''\, dz\right\},$$

$$q_b'' = q''\left[\frac{h_l - h_{ld}}{h_f - h_{ld}}\right],$$

$$q_{cond}'' = \begin{cases} H_0\left(\frac{h_{fg}}{v_{fg}}\right)\left(\frac{A}{p_H}\right)\langle\alpha\rangle(T_{sat} - T_l), & \text{for } h_l \geqslant h_{ld}, \\ 0, & \text{for } h_l < h_{ld}, \end{cases}$$

$$\varepsilon = \frac{\rho_l(h_f - h_l)}{\rho_g h_{fg}},$$

$$T_l = F_1(h_l); \quad \rho_l = F_2(T_l),$$

$$h_l = \left\{\frac{h_{avg} - h_g x_{avg}}{1 - x_{avg}}\right\},$$

$$\rho_{avg} = \frac{\rho_g}{\left\{\frac{\rho_g}{\rho_l}(1 - x_{avg}) + x_{avg}\right\}},$$

$$\langle\alpha\rangle = \frac{x_{avg}}{\left\{\left(\frac{\rho_g}{\rho_l}\right)(1 - x_{avg}) + x_{avg}\right\}} = \frac{x_{avg}\rho_{avg}}{\rho_g}.$$

Calculation of ψ and i_b

$$\mu_{avg} = \mu_l \exp\left[2.55\alpha_{avg}\Big/\left(1 - \frac{39\langle\alpha\rangle}{64}\right)\right],$$

$$Re = \frac{GD}{\mu_{avg}}$$

$$D_p = 0.015\left(\frac{8\sigma D_h g_c \rho_{avg}}{f' G^2}\right)^{1/2},$$

$$i_b = 0.790\left(\frac{GD}{\mu_{avg}}\right)^{-0.1}\left(\frac{D_p}{D}\right)^{0.6}\left[1 + a\frac{(\rho_l - \rho_g)}{\rho_g}\right],$$

$$a = 0.135 \quad \text{if} \quad G \leqslant 9.7 \times 10^6 \text{ kg m}^{-2} \text{ h}^{-1}$$

$$a = 0.135\left(\frac{G}{9.7 \times 10^6}\right)^{-0.3}$$

for

$$G > 9.7 \times 10^6 \text{ kg m}^{-2} \text{ h}^{-1}$$

$$\sigma_{v'} = \frac{i_b G}{\bar{\rho}} = i_b\left[\frac{G}{\rho_l} + \left(\frac{G}{\rho_g} - \frac{G}{\rho_l}\right)x_{avg}\right],$$

$$v_{11} = \frac{q''_b}{\rho_g h_{fg}},$$

$$\psi = \left\{\frac{1}{\sqrt{2\pi}}\exp\left[-\frac{1}{2}\left(\frac{v_{11}}{\sigma_{v'}}\right)^2\right] - \frac{1}{2}\left(\frac{v_{11}}{\sigma_{v'}}\right)\text{erfc}\left(\frac{1}{\sqrt{2}}\frac{v_{11}}{\sigma_{v'}}\right)\right\}.$$

Calculation of x_1, ρ_1 based on $\alpha_2 = 0.82$

$$s = 5.5D_p,$$

$$\rho_1 = \rho_{avg}x\frac{r_0^2}{(r_0 - s)^2} - \rho_2\frac{2\left(r_0 - \frac{s}{2}\right)s}{(r_0 - s)^2},$$

$$\alpha_1 = \frac{(\rho_{11} - \rho_1)}{(\rho_{11} - \rho_g)},$$

$$x_1 = \frac{\alpha_1\rho_g}{\rho_1}.$$

q'' is the critical heat flux when the LHS and RHS of equation (A1) are equal. If equality not obtained, readjust assumed q'' and repeat process.

PREVISION DU FLUX THERMIQUE CRITIQUE DANS UN ECOULEMENT AVEC EBULLITION A FAIBLE QUALITE

Résumé—Un calcul théorique du CHF est développé pour l'écoulement à grande vitesse dans les tubes. L'échange turbulent entre la couche chargée de bulles et la région du coeur est pris comme mécanisme limitatif. Un bon accord est obtenu entre les prévisions et les données de l'expérience pour l'eau s'écoulant dans des tubes chauffés uniformément ou non. La procédure développée pour l'eau fournit aussi des résultats conformes à l'expérience pour chacun des quatre autres fluides considérés.

VORAUSBERECHNUNG DER KRITISCHEN WÄRMESSTROMDICHTE BEI STRÖMUNGSSIEDEN UND GERINGEM DAMPFGEHALT

Zusammenfassung—Eine theoretische Methode zur Vorausberechnung der kritischen Wärmestromdichte für Hochgeschwindigkeitsströmung in Rohren wurde entwickelt. Der turbulente Austausch zwischen der Blasenschicht und dem Kern wurde als bestimmender Mechanismus herangezogen. Gute Übereinstimmung wurde zwischen vorausberechneten und experimentellen Daten für Wasser in gleichmäßig und ungleichmäßig beheizten Rohren festgestellt. Es zeigte sich, daß die für Wasser entwickelte Berechnungsmethode für vier andere ebenfalls untersuchte Fluide Ergebnisse liefert, die in guter Übereinstimmung mit den Experimenten stehen.

РАСЧЕТ КРИТИЧЕСКОГО ТЕПЛОВОГО ПОТОКА ДЛЯ ТЕЧЕНИЙ С КИПЕНИЕМ ПРИ НИЗКИХ ЗНАЧЕНИЯХ ПАРОСОДЕРЖАНИЯ

Аннотация—Теоретически рассчитан критический тепловой поток (КТП) для высокоскоростного течения в трубах. В качестве лимитирующего механизма принят турбулентный обмен между пузырьковым слоем и сердцевинной частью потока. Получено хорошее соответствие между расчетными и экспериментальными данными для течения воды в трубах с однородным и неоднородным нагревом. Обнаружено, что методика расчета, примененная для воды, дает результаты, согласующиеся с экспериментальными данными, полученными для каждой из четырех других исследованных жидкостей.